Classical interpretation of nonrelativistic quark potential model: Color charge definition and meson mass-radius relationship*

Zhiguang Tan (谭志光)[1†] Youneng Guo (郭有能)[1‡] Shengjie Wang (王胜杰)[1] Hua Zheng (郑华)[2§]

[1]School of Electronic Information and Electrical Engineering, Changsha University, Changsha 410003, China
[2]School of Physics and Information Technology, Shaanxi Normal University, Xi'an 710119, China

Abstract: Quantum chromodynamics (QCD) is a fundamental theory describing quark interactions. Thus far, various quark models based on QCD have been widely used to study the properties of hadrons, including their structures and mass spectra. However, unlike quantum electrodynamics and Bohr's model of the hydrogen atom, a direct classical analogy is lacking for hadronic structures. This paper presents a classical interpretation of the nonrelativistic quark potential model, providing a more intuitive and visualizable description of strong interactions through the quantitative formulation of color charge and color flux. In addition, we establish the relationship between meson mass and its structural radius in the nonrelativistic framework and estimate key parameters of our model using available data from $\eta_b(1S)$ and $\Upsilon(1S)$. Subsequently, we extend this relationship to a broader range of excited meson states and obtain their structural radii, which show good agreement with the root mean square radius or charge radius predicted by QCD calculations.

Keywords: meson structure, mass spectra and radius, quark potential model, interaction, color charge

DOI: 10.1088/1674-1137/ae28e9 **CSTR:** 32044.14.ChinesePhysicsC.50033106

I. INTRODUCTION

When the Schrödinger equation

$$\nabla^2\Psi+\frac{2m}{\hbar^2}[E-V(r)]\Psi=0 \tag{1}$$

is solved to obtain the eigenenergies and mass spectra of a meson system composed of a pair of positive and negative quarks, the potential function $V(r)$ of the system is pivotal, *i.e.*, the so-called quark potential model [1−3]. Among them, the Cornell potential [4] proposed in the 1980s has performed effectively, and most current potential models based on it incorporate various improvements or extensions [5, 6]. It is expressed as [4]

$$V(r)=-\frac{a}{r}+br, \tag{2}$$

where a and b are two positive parameters. The first term in Eq. (2) is the Coulomb-like potential, whereas the second term considers the property of quark confinement. Thus, it is very difficult to separate a pair of attractive quarks. Solving Eq. (1) to obtain the mass eigenstates and quantum properties of hadrons constitutes an approach to study the nature of those hadrons [7, 8]. To obtain results close to experimental measurements, not only should the parameters be adjusted but the expression for the potential function should also be extended. In Refs. [9, 10], the potential has been extended to a more general form

$$V(r)=ar^2+br-\frac{c}{r}+\frac{d}{r^2}+e. \tag{3}$$

However, except for the two terms in Eq. (2), no physically reasonable explanations have been provided for the origins of the other terms in Eq. (3).

According to a classical interpretation, quantum numbers that describe the properties of hadrons [11] are inherently linked to their internal structure. Therefore, the interaction between quarks should be determined by their color charge values, relative positions, motion states, and spin orientations. This study aims to identify physical origins for each term in the potential model, Eq. (3), and provide a classical description of quark interactions.

The paper is organized as follows: In Sec. II, we introduce the concept of unit color charge and discuss the

Received 4 June 2025; Accepted 4 December 2025; Accepted manuscript online 5 December 2025

* Supported in part by the Department of Education (21A0541) and Natural Science Foundation (2025JJ50382) of Hunan province, China

† E-mail: tanzg@ccsu.edu.cn
‡ E-mail: guoxuyan2007@163.com
§ E-mail: zhengh@snnu.edu.cn

interaction between two stationary color charges in vacuum. Further, we provide the rule for the dot product of two color charges, along with the basic function, which corresponds to the Coulomb-like term in the potential Eq. (3). Section III explains the inverse square term in the potential by introducing concepts of color flow and color magnetic field. Section IV addresses the harmonic oscillator potential arising from the spin, which corresponds to the other three terms in Eq. (3). In Sec. V, we estimate the relevant model parameters and present our numerical results based on the classical description of meson structures, comparing them with data in the literature from potential models. Finally, a brief summary and discussion are given in Sec. VI.

II. INTERACTION BETWEEN A PAIR OF STATIONARY QUARKS IN VACUUM

To provide a classical description of the interaction between a pair of quarks, we first define three fundamental color charges c_r, c_g, c_b and their corresponding anti-color charges $c_{\bar{r}}, c_{\bar{g}}, c_{\bar{b}}$ as follows

$$\begin{aligned} &c_r \equiv \mathrm{e}^{\theta \mathrm{i}}, \quad c_{\bar{r}} \equiv \mathrm{e}^{(\theta+\pi)\mathrm{i}} = -c_r; \\ &c_g \equiv \mathrm{e}^{(\theta+\frac{2\pi}{3})\mathrm{i}}, \quad c_{\bar{g}} \equiv \mathrm{e}^{(\theta-\frac{\pi}{3})\mathrm{i}} = -c_g; \\ &c_b \equiv \mathrm{e}^{(\theta-\frac{2\pi}{3})\mathrm{i}}, \quad c_{\bar{b}} \equiv \mathrm{e}^{(\theta+\frac{\pi}{3})\mathrm{i}} = -c_b; \end{aligned} \tag{4}$$

with $0 \le \theta < \pi$ in the complex plane. In fact, only a relative meaning exists between r, g, and b. The modulus of each color charge is 1, and therefore it is also referred to as the unit color charge. Further, we can represent them in the form of unit vectors in the unit circle, as shown in Fig. 1.

Obviously, they satisfy

$$\vec{c}_i + \vec{c}_{\bar{i}} = 0, \tag{5}$$

$$\vec{c}_r + \vec{c}_g + \vec{c}_b = 0, \tag{6}$$

with $i = r, g, b$, which ensures the color neutrality of mesons and baryons. Color charges are quantized; therefore, they can only be integer mutiples of the three unit color charges aforementioned. The color charges can be added together as

$$C = \sum_{i=r,g,b} (n_i c_i + n_{\bar{i}} c_{\bar{i}}). \tag{7}$$

For example, a di-quark composed of a red color charge and a blue color charge results in an anti-green color charge, which enables the existence of particles with color charges other than unit color charges. The interaction between a pair of stationary color charges in vacuum is Coulomb-like and defined as

$$\boldsymbol{F}_{C_1C_2} = Z\frac{C_1 \cdot C_2}{r^3}\boldsymbol{r}. \tag{8}$$

Here, Z is the vacuum color gravitational constant and has units of Nm^2. The dot product of two color charges is defined as the dot product of the vectors represented by the two color charges. Therefore, the dot product $c_{ij} = \vec{c}_i \cdot \vec{c}_j$ between two unit color charges is the matrix element of the matrix

$$CC = Q\begin{bmatrix} 1 & -1/2 & -1/2 \\ 1/2 & 1 & -1/2 \\ 1/2 & 1/2 & 1 \end{bmatrix}, \tag{9}$$

with $Q = -1$ for a quark and an anti-quark, and $Q = 1$ otherwise. This definition is similar to the one in Ref. [12]. As shown in Fig. 2, one can verify that the total interaction between a blue quark (or antiquark) and a three quark cluster (with a total color charge of zero) is zero.

$$F = \sum_{i}^{r,g,b} Z\frac{\pm c_b \cdot c_i}{r^2} = Z\frac{\sum_i^{r,g,b} \pm c_b \cdot c_i}{r^2} = 0. \tag{10}$$

Obviously, when considering infinity as the zero point of the color potential energy, that between the two color charges can be calculated by

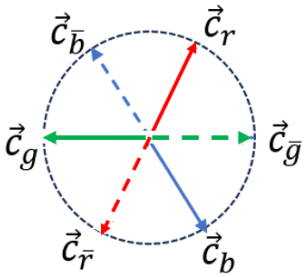

Fig. 1. (color online) Vector representation of unit color charge.

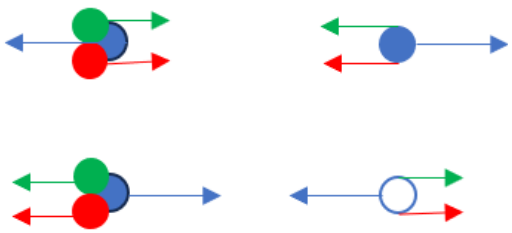

Fig. 2. (color online) Interaction between a blue quark(anti-quark) and a three-quark cluster.

$$E_p = \int_r^{\infty} \frac{F_{C_1C_2}}{r^2}\mathrm{d}r = -Z\frac{C_1\cdot C_2}{r}. \tag{11}$$

When $C_1 = -C_2$ and $|C_1| = 1$, the result above corresponds to the third term in Eq. (3), which is the Coulomb-like term.

III. COLOR MAGNETIC FIELD FROM THE MOTION OF COLOR CHARGE

The collective motion of color charges generates color flow. Similar to the electrical current intensity, the current intensity of color flow is defined as the amount of color charge flowing through a cross-section per unit time.

$$I_c = \frac{|\Delta C|}{\Delta t} = \frac{|\sum_{i=r}^{b}(n_i - n_{\bar{i}})c_i|}{\Delta t}. \tag{12}$$

It is assumed that color flow can generate a color magnetic field, modeled after Biot Savart's law

$$\boldsymbol{B}_c = \int_l T\frac{I_c\mathrm{d}\boldsymbol{l}\times\boldsymbol{R}}{R^3}. \tag{13}$$

Here, T is the parameter under vacuum, and its value needs to be measured directly or indirectly through experiments. For example, consider the color magnetic field generated by a circular color flow. As shown in Fig. 3, assume that the radius of the circular color current is a and the color current intensity is I_c. The following formula can be derived by simulating the magnetic field generated by a circular current [13]

$$\begin{aligned} B_{cx} &= TI_c a r\cos\theta\int_0^{2\pi}\frac{\cos\varphi}{(r^2+a^2-2ra\sin\theta\cos\varphi)^{3/2}}\mathrm{d}\varphi,\\ B_{cy} &= 0,\\ B_{cz} &= TI_c\int_0^{2\pi}\frac{a^2-ar\sin\theta\cos\varphi}{(r^2+a^2-2ra\sin\theta\cos\varphi)^{3/2}}\mathrm{d}\varphi. \end{aligned} \tag{14}$$

For points on the color flow plane, $\theta = \pi/2, \sin\theta = 1$, and $\cos\theta = 0$; therefore, $B_{cx} = B_{cy} = 0$ and

$$\begin{aligned} B_{cz} &= TI_c\int_0^{2\pi}\frac{a^2-ar\cos\varphi}{(r^2+a^2-2ra\cos\varphi)^{3/2}}\mathrm{d}\varphi\\ &= 2TI_c\left[\frac{1}{a-r}E(k)+\frac{1}{a+r}K(k)\right]\\ &= 2TI_cX(a,r). \end{aligned} \tag{15}$$

Here, $E(k)$ and $K(k)$ represent elliptic functions ellipticE and ellipticK, respectively, with $k = 2\sqrt{ar}/(a+r)$. The color magnetic field diverges on the color flow circular line, as shown in Fig. 4.

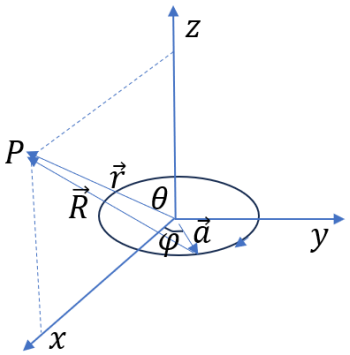

Fig. 3. (color online) Calculation of the color magnetic field generated by a circular color flow.

For different radii of circular currents, we obtain a simple explanatory formula for the inner and outer color magnetic fields of the circle through segmented fitting. Here, X_i and X_o represent the values of $B_{cz}/(2TI_c)$ inside and outside the circle, respectively.

$$\begin{aligned} a = 0.5,\ & X_i = 1.2215\frac{1}{a-r} + 9.9248(a-r),\\ & X_o = -0.8433\frac{1}{r-a} + 5.0440(r-a);\\ a = 0.6,\ & X_i = 1.2001\frac{1}{a-r} + 7.0576(a-r),\\ & X_o = -0.8593\frac{1}{r-a} + 3.6412(r-a);\\ a = 0.7,\ & X_i = 1.1833\frac{1}{a-r} + 5.2816(a-r),\\ & X_o = -0.8717\frac{1}{r-a} + 2.7549(r-a);\\ a = 0.8,\ & X_i = 1.1696\frac{1}{a-r} + 4.1042(a-r),\\ & X_o = -0.8817\frac{1}{r-a} + 2.1587(r-a);\\ a = 0.9,\ & X_i = 1.1583\frac{1}{a-r} + 3.2828(a-r),\\ & X_o = -0.8900\frac{1}{r-a} + 1.7381(r-a);\\ a = 1.0,\ & X_i = 1.1487\frac{1}{a-r} + 2.6866(a-r),\\ & X_o = -0.8970\frac{1}{r-a} + 1.4301(r-a). \end{aligned} \tag{16}$$

The color magnetic field energy stored in a color flow ring can be calculated as

$$E_{Bc} = \frac{1}{2}I_c\int \boldsymbol{B}_c\cdot\mathrm{d}\boldsymbol{S} = TI_c^2\int_0^a X_i 2\pi r\mathrm{d}r. \tag{17}$$

As the value of T is yet to be determined, Fig. 5

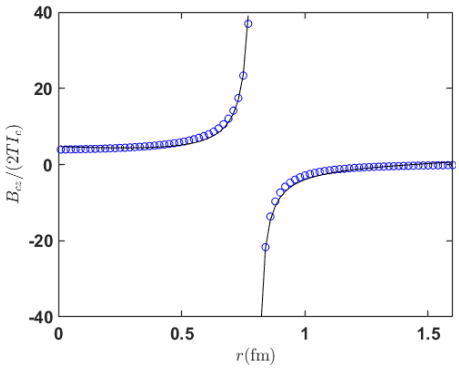

Fig. 4. (color online) Distribution of the color magnetic field generated by a circular color flow in the color flow plane. The small circles in the figure are calculated according to Eq. (15), and the solid lines are fitted by Eq. (16).

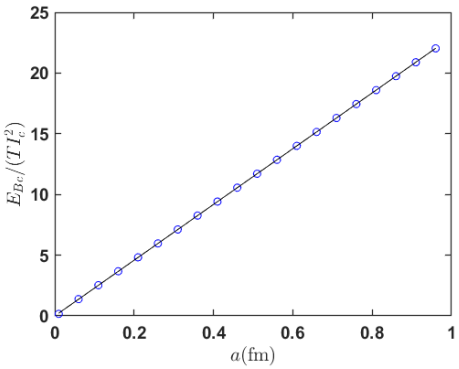

Fig. 5. (color online) The open circles are the results calculated by Eq. (17). The solid line is the fit by Eq. (18).

provides the calculated values and fitting relationships of $\frac{E_{Bc}}{TI_c^2}$ versus a, using

$$\frac{E_{Bc}}{TI_c^2} = 22.97a. \tag{18}$$

Now, we can apply our scenario to mesons. When one quark orbits another quark in a circular motion with a radius r, its equivalent color flow intensity is

$$I_c = |c|\frac{v}{2\pi r} = \frac{v}{2\pi r}. \tag{19}$$

Considering the centripetal force provided by the color charge force,

$$Z\frac{1}{r^2} = m\frac{v^2}{r}, \tag{20}$$

and the color magnetic energy stored in the meson is

$$E_{Bc} = 22.97TI_c^2 r = 0.5818T\frac{Z}{mr^2}. \tag{21}$$

This is the fourth term in the potential energy Eq. (3), which is inversely proportional to the square of the distance.

IV. HARMONIC OSCILLATOR POTENTIAL ORIGINATED FROM SPIN

In quantum mechanics, spin is an intrinsic property of particles. However, in classical terms, we propose that particle spin is an external manifestation of its internal structure. We assume that the quark color charge undergoes circular motion around its own central axis, which is equivalent to a circular color flow ring, possessing a colored magnetic moment. For a meson system composed of a pair of positive and negative quarks, as shown in Fig. 6, the color magnetic moments of the two quarks must be coplanar because of the effect of the chromomagnetic torque. Consequently, their spin orientations can only have two states: parallel or antiparallel. During their respective rotations, when the directions of the two color flows are parallel, the spin interaction is attractive. The spin interaction is repulsive when the directions are antiparallel. If the color flow directions are perpendicular to each other, no force acts between them.

Therefore, spin induced interactions can be described by a harmonic oscillator, whose dynamic equilibrium position lies along the circumference of the orbital motion of the quark, as

$$F_{S_1S_2} = -k(r'-r) = -\frac{1}{2}m\omega^2(r'-r). \tag{22}$$

Here, k and ω represent the elastic coefficient and angular frequency, respectively. The total energy of the oscillator is

$$E_s = \frac{1}{2}kA^2 = \frac{1}{2}k(r_m - r)^2. \tag{23}$$

Expanding the right-hand side of the above equation yields the remaining three terms of Eq. (3). Owing to the extremely small size of $r_m - r$ (comparable to the radius of quarks), the vibrational energy is expressed using the quantum mechanical harmonic oscillator energy formula

$$E_s = (L+\frac{1}{2})\hbar\omega_{nL}, \quad (L = 0,1,2,\cdots,n-1). \tag{24}$$

The top row in Fig. 7 represents the state where two quarks have parallel spins, while the bottom row represents the state with antiparallel spins, *i.e.* $S_1+S_2 = 0,\ 1$. Clearly, the stationary orbital motion period must satisfy a specific relationship with the spin period. As shown in Fig. 7, for a meson system to be in a stable state, the peri-

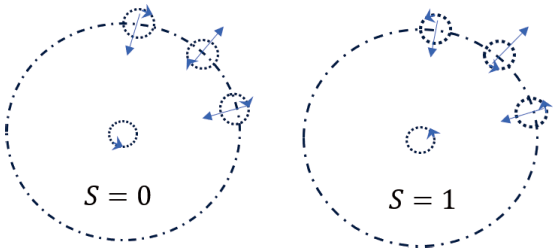

Fig. 6. (color online) Schematic of spin interaction. When the color flow is parallel, they are attracted to each other. When it is antiparallel, they are repelled.

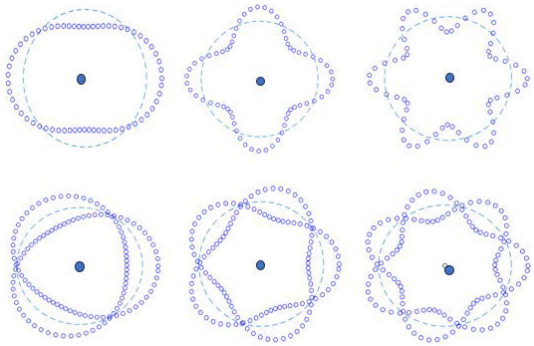

Fig. 7. (color online) Meson mechanics structure diagram with $n=1,2,3$ from the left to the right. The top row corresponds to $S=0$, while the bottom row is for $S=1$.

od of quark circular motion $T_\theta = 2\pi r/v$ must be an odd (for $S=0$) or even (for $S=1$) multiple of the vibration half-period, *i.e.*,

$$\frac{2\pi r_{nL}}{v_{nL}} = \begin{cases} (2n-1)\dfrac{\pi}{\omega_{nL}}, & (S=0), \\ 2n\dfrac{\pi}{\omega_{nL}}, & (S=1), \end{cases} \qquad n=1,2,\cdots \tag{25}$$

According to Eq. (20), one can obtain

$$r_{nL}^3 = \begin{cases} (n-\dfrac{1}{2})^2\dfrac{Z}{m\omega_{nL}^2}, & (S=0), \\ n^2\dfrac{Z}{m\omega_{nL}^2}, & (S=1). \end{cases} \tag{26}$$

The terms ω_{nL} here do not represent the angular velocity of orbital motion, *i.e.*, $\omega_{nL} \neq v_{nL}/r_{nL}$.

V. VALUES OF Z AND T AND RESULTS

Due to color confinement, it is impossible to directly measure the values of Z and T by measuring the forces between two free quarks or two color currents. Instead, we can only estimate their values using the masses and radii of certain hadrons measured experimentally.

In the center of the mass frame of a meson, the mass of the meson can be calculated as [14, 15]

$$M_{nL} = M_Q + M_{\bar{q}} + E_{nL}. \tag{27}$$

Here, E_{nL} includes the previously mentioned E_p, E_{Bc}, E_s, and the kinetic energy $E_k = \frac{1}{2}mv^2 = \frac{Z}{2r}$, where the reduced mass is given by

$$m = \frac{M_Q M_{\bar{q}}}{M_Q + M_{\bar{q}}}. \tag{28}$$

Therefore, for a meson in a state with quantum number n and L, the classical calculation of its mass can be expressed as

$$M_{nL} = M_Q + M_{\bar{q}} - \frac{Z}{2r_{nL}} + 0.5818T\frac{Z}{mr_{nL}^2} + (L+\frac{1}{2})(n-\frac{1}{2}\delta_{S0})\sqrt{\frac{Z}{mr_{nL}^3}}. \tag{29}$$

For the ground state radius r_{10} and mass M_{10}, we have

$$r_{10}^3 = \frac{Z}{4m\omega_{10}^2}\ (S=0) \quad \text{or} \quad \frac{Z}{m\omega_{10}^2}\ (S=1), \tag{30}$$

$$M_{10} = M - \frac{Z}{2r_{10}} + 0.5818T\frac{Z}{mr_{10}^2} + \frac{1}{2}\sqrt{\frac{\frac{1}{4}(1)Z}{mr_{10}^3}}. \tag{31}$$

In Eq. (31), coefficients 1/4 and 1 under the square root correspond to the cases of spins 0 and 1, respectively. The values of Z and T are universal, which enables us to use a small amount of experimental data to deduce their values. Then, we use the obtained values of Z and T to calculate the results for other mesons and test our model using the experimental data.

The previous discussion did not consider relativistic effects, which may require corrections for light meson systems. For heavy mesons, relativistic effects are likely less significant, and therefore we use heavy meson data to calculate Z and T.

Unfortunately, directly measuring meson radii is very challenging because of the current experimental limitations. However, model calculations of meson sizes have gained significant interest among scientists. Currently, two important radii are used to describe the size of meson systems: the so-called root mean square (r.m.s.) radius $\langle r_{\rm rms}^2\rangle$ [16, 17] and charge radius $\langle r_E^2\rangle$ [18], which are defined as

$$\langle r^2_{\rm rms}\rangle = \int_0^\infty r^2[\psi(r)]^2 {\rm d}r, \tag{32}$$

$$\langle r^2_E\rangle = -6\frac{{\rm d}^2}{{\rm d}Q^2}eF(Q^2)\big|_{Q^2=0}, \tag{33}$$

where $\psi(r)$ and $F(Q^2)$ represent the radial wave function and form factor of the meson, respectively [19, 20]. According to the calculations in Refs. [21, 22], the root mean square (r.m.s.) radius of the $\Upsilon(1S)$ state is approximately 0.2671 fm. Ref. [23], through a comprehensive contact interaction analysis, determined that the ground state charge radius of the pseudoscalar meson η_b is about 0.07 fm.

Now, we use the data of these two mesons to determine parameters Z and T. The mass data of these mesons are obtained from the Particle Data Group (PDG), while the mass of the constituent b quark is taken as $m_b = 4.95$ GeV, which is consistent with Refs. [21, 22]. These data are listed in Table 1. The obtained values of Z and T are

$$Z = 2.33, \quad T = 0.375. \tag{34}$$

In the above discussions, we adopted the natural units commonly used in high-energy physics, where $\hbar = c = 1$, with GeV as the basic unit. In the International System of Units (SI), $c = 2.998\times10^8$ m/s, $\hbar c \approx 0.197$ GeV·fm. According to Eqs. (8) and (18), the units of Z and T should be $[Z] = ML^3T^{-2}$ and $[T] = ML$, respectively. Thus,

$$\begin{aligned} Z &= 2.33\times\frac{\rm GeV}{c^2}\times(0.197{\rm fm})^3\times\frac{c^2}{(0.197{\rm fm})^2} \\ &= 7.35\times10^{-26}Nm^2, \\ T &= 0.375\times\frac{\rm GeV}{c^2}\times(0.197{\rm fm}) \\ &= 1.32\times10^{-43}Ns^2. \end{aligned} \tag{35}$$

Comparing the magnitude of gravitational forces between a pair of quark and antiquark that are 1 fm apart (with mass and charge of $m_b = m_{\bar b} = 4.95$ GeV, $q_b = -q_{\bar b} = -1/3e$)

$$F_m = G\frac{m_b m_{\bar b}}{r^2} = 5.16\times10^{-33}N, \tag{36}$$

$$F_e = k\frac{q_b q_{\bar b}}{r^2} = 2.56\times10N, \tag{37}$$

$$F_c = Z\frac{c_i c_{\bar i}}{r^2} = 2.01\times10^4N, \tag{38}$$

Table 1. Meson data taken from PDG [24] and Refs. [21, 23].

$n^{2S+1}L_j$	Name	$q\bar q'$	$\sqrt{\langle r_1\rangle^2}$/fm	M/GeV
1^1S_0	$\eta_b(1S)$	$b\bar b$	0.070	9.3987
1^3S_1	$\Upsilon(1S)$	$b\bar b$	0.268	9.4604

reveals that the strong interaction based on color charge is considerably greater than those of the other two, which is consistent with the hiearchy of force magnitudes. We use the meson masses provided by the PDG [24] as inputs. By applying Eq. (29), we calculate the corresponding meson radii and compare them with the results from other models, as indicated in Table 2.

Table 2 shows that some of results are in good agreement with the results in the literature. Existing studies on meson radius calculations employ various models [21, 23, 28−30], each with its own set of parameters, and most studies focus only on the lowest few states. Our model also relies on data from a few mesons; however, this can be attributed to the current inability to experimentally measure Z and T. Once these two values are determined scientifically, a predictable relationship between meson mass and its structural radius can be established. As shown in Fig. 8, we present the mass-radius relationship for several quantum states of $b\bar b$ mesons based on Eq. (29), which is of significant importance for understanding hadron structures. We observe an anomaly in the n^3S_1 state series, particularly in the $\Upsilon(nS)$ mesons. In general, the radius of the excited state of the meson is typically larger than that of its ground state. Our analysis suggests that this anomaly is related to spin-dependent terms: for heavy-flavor quarks, the effect of spin energy is significant. Spin-induced vibrations intensify with an increasing energy level, while causing the parameter ω to increase. According to Eq. (26), this leads to an increase in v. When the angular momentum L remains constant, this leads to a reduction in radius r; this will be experimentally examined in future.

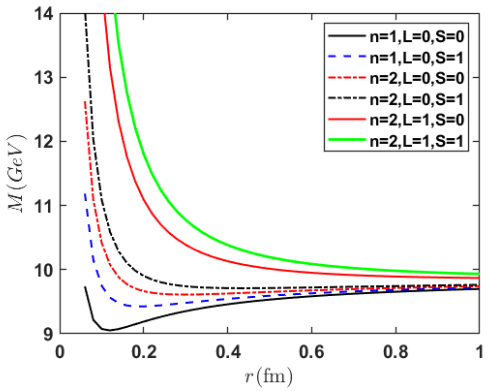

Fig. 8. (color online) According to Eq. (29), the relationship between the mass and radius of a heavy meson composed of a bottom quark (b) and an anti-bottom quark ($\bar b$).

Table 2. Results of our model for the particles in PDG. The last column contains reference values from the literature.

name	$q\bar{q}'$	state	M/GeV	ω	r_{nL}/fm	$\sqrt{r^2}$[Ref.]
$\eta_b(1S)$	$b\bar{b}$	1^1S_0	9.3987	0.9093	0.0700	0.07 [23]
$\Upsilon(1S)$	$b\bar{b}$	1^3S_1	9.4604	0.8352	0.2680	0.2671 [23]
$\chi_{b0}(1P)$	$b\bar{b}$	1^3P_0	9.8594	0.2972	0.4340	0.39 [23]
$\chi_{b1}(1P)$	$b\bar{b}$	1^3P_1	9.8928	0.3586	0.3830	
$h_b(1P)$	$b\bar{b}$	1^1P_1	9.8993	0.3694	0.3755	
$\chi_{b2}(1P)$	$b\bar{b}$	1^3P_2	9.9122	0.3910	0.3615	
$\eta_b(2S)$	$b\bar{b}$	2^1S_0	9.9987	2.8256	0.1268	
$\Upsilon(2S)$	$b\bar{b}$	2^3S_1	10.0233	2.3623	0.1730	
$\Upsilon_2(1D)$	$b\bar{b}$	1^3D_2	10.1637	0.3019	0.4295	
$\chi_{b0}(2P)$	$b\bar{b}$	2^3P_0	10.2325	0.5209	0.4740	
$\chi_{b1}(2P)$	$b\bar{b}$	2^3P_1	10.2555	0.5448	0.4600	
$h_b(2P)$	$b\bar{b}$	2^1P_1	10.2598	0.6445	0.3395	
$\chi_{b2}(2P)$	$b\bar{b}$	2^3P_2	10.2687	0.5575	0.4530	
$\eta_b(3S)$	$b\bar{b}$	3^1S_0	10.3268	2.9857	0.1718	
$\Upsilon(3S)$	$b\bar{b}$	3^3S_1	10.3552	2.7877	0.2030	
$\chi_{b1}(3P)$	$b\bar{b}$	3^3P_1	10.5134	0.6839	0.5180	
$\chi_{b2}(3P)$	$b\bar{b}$	3^3P_2	10.5240	0.6939	0.5130	
$\eta_b(4S)$	$b\bar{b}$	4^1S_0	10.5397	3.1094	0.2092	
$\Upsilon(4S)$	$b\bar{b}$	4^3S_1	10.5794	3.0422	0.2320	
$\eta_b(5S)$	$b\bar{b}$	5^1S_0	10.8202	3.5592	0.2261	
$\Upsilon(5S)$	$b\bar{b}$	5^3S_1	10.8761	3.5696	0.2420	
$\eta_c(1S)$	$c\bar{c}$	1^1S_0	2.9839	0.7948	0.2090	0.20 [23]
$J/\psi(1S)$	$c\bar{c}$	1^3S_1	3.0969	0.9675	0.2910	0.37 [27]
						0.28 [28]
$\chi_{c0}(1P)$	$c\bar{c}$	1^3P_0	3.4147	0.4539	0.4820	0.43 [23]
$\chi_{c1}(1P)$	$c\bar{c}$	1^3P_1	3.5107	0.5368	0.4310	
$h_c(1P)$	$c\bar{c}$	1^1P_1	3.5254	0.6262	0.2450	
$\chi_{c2}(1P)$	$c\bar{c}$	1^3P_2	3.5662	0.5839	0.4075	
$\eta_c(2S)$	$c\bar{c}$	2^1S_0	3.6375	2.1065	0.2270	0.386 [28]
$\psi(2S)$	$c\bar{c}$	2^3S_1	3.6861	2.1773	0.2690	0.387 [28]
$\psi(3770)$	$c\bar{c}$	$2^3P_{0,1}$	3.7737	0.6569	0.5980	
$\psi_2(3823)$	$c\bar{c}$	2^3P_2	3.8237	0.6967	0.5750	
$\psi_3(3842)$	$c\bar{c}$	2^3P_3	3.8427	0.7715	0.5670	
$\chi_{c1}(3872)$	$c\bar{c}$	2^3P_1	3.8717	0.7347	0.5550	
$\chi_{c0}(3915)$	$c\bar{c}$	2^1P_0	3.9217	0.8122	0.4285	
$\chi_{c2}(3930)$	$c\bar{c}$	2^3P_2	3.9225	0.7741	0.5360	
B_c^+	$c\bar{b}$	1^1S_0	6.2745	0.0920	0.7650	0.38 ~ 1.09 [25]
$B_c^+(2S)$	$c\bar{b}$	2^1S_0	6.8712	0.2290	0.1900	0.17 [23]
B_s^0	$s\bar{b}$	1^1S_0	5.3669	0.4514	0.3680	0.24 [23]
B_s^*	$s\bar{b}$	1^3S_1	5.5154	0.7485	0.4170	
$B_{s1}(5830)^0$	$s\bar{b}$	1^3P_1	5.8286	0.4359	0.5980	

Continued on next page

Table 2-continued from previous page

name	$q\bar{q}'$	state	M/GeV	ω	r_{nL}/fm	$\sqrt{r^2}$[Ref.]
$B^*_{s2}(5840)^0$	$s\bar{b}$	1^3P_2	5.8399	0.4448	0.5900	
D^+	$c\bar{d}$	1^1S_0	5.2793	2.5089	0.1370	0.10 ~ 0.42 [26]
D^0	$c\bar{u}$	1^1S_0	1.8648	0.3175	0.5435	0.14 ~ 0.55 [26]
D_s^+	$c\bar{s}$	1^1S_0	1.9683	0.3607	0.4535	0.10 ~ 0.4 [26]
η'	$s\bar{s}$	1^1S_0	0.9578	0.2934	0.5990	0.5 [26]

VI. SUMMARY

We propose a numerical representation method for the color properties of quarks, which facilitates the convenient superposition of color charges and predicts the existence of multi-color-charge states. In analogy with classical electromagnetic field theory, we introduce novel concepts such as "color force," "color current," and "color magnetic field." Further, we explore the structure of mesons composed of quark-antiquark pairs using Bohr's model of the hydrogen atom. Using masses of $\eta_b(1S)$ and $\Upsilon(1S)$ from the PDG and their radii from literature, we estimate the fundamental parameters Z for color charge interactions and T for color current interactions in our model. With the determined values, we calculate the masses and radii for several other mesons and compare the results with available literature, finding close agreements. We admit that more precise calculations of these physical quantities can be achieved using the QCD theory. Further, we believe that the classical description of inter-quark interactions in this paper presents a simple and intuitive picture worthy of discussion.

References

[1] C. Semay and B. Silvestre-Brac., Nucl. Phys. A **618**(4), 455 (1997)
[2] K. Watanabe, Phys. Rev. D **105**(7), 074510 (2022)
[3] Z. Zhao, K. Xu, A. Limphirat *et al.*, Phys. Rev. D **109**(1), 016012 (2024)
[4] E. Eichten, K. Gottfried, T. Kinoshita *et al.*, Phys. Rev. D **21**(1), 203 (1980)
[5] A. I. Ahmadov, K. H. Abasova, M. S. Orucova, Advances in High Energy Phys. **2021**(1), 1861946 (2021)
[6] L. P. Fulcher, Z. Chen, and K. C. Yeong, Phys. Rev. D **47**(9), 4122 (1993)
[7] F. X. Liu, R. H. Ni, X. H. Zhong *et al.*, Phys. Rev. D **107**(9), 096020 (2023)
[8] T. Y. Li, L. Tang, Z. Y. Fang *et al.*, Phys. Rev. D **108**(3), 034019 (2023)
[9] V. Kumar, R. M. Singh, S. B. Bhardwaj *et al.*, Mod. Phys. Lett. A **37**(02), 2250010 (2022)
[10] M. Abu-Shady and E. M. Khokha, Int. J. Mod. Phys. A **36**(29), 2150195 (2021)
[11] Z. G. Tan, S. J. Wang, Y. N. Guo *et al.*, Nucl. Sci. Tech. **35**(8), 144 (2024)
[12] Z. G. Tan and C. B. Yang, Int. J. Mod. Phys. E **24**(06), 1550044 (2015)
[13] J. M. Griffith and G. W. Pan, IEEE Transactions on Magnetics **47**(8), 2029 (2011)
[14] M. Abu-Shady, T. A. Abdel-Karim, and S. Y. Ezz-Alarab, Journal of the Egyptian Mathematical Society **27**(1), 1 (2019)
[15] R. Rani, S. B. Bhardwaj, and F. Chand, Comm. in Theor. Phys. **70**(2), 179 (2018)
[16] N. Akbar, B. Masud, and S. Noor, Eur. Phys. J. A **47**, 1 (2011)
[17] A. M. Yasser, G. S. Hassan, and T. A. Nahool, J. Mod. Phys. **5**(17), 1938 (2014)
[18] K. U. Can, G. Erkol, M. Oka *et al.*, Phys. Lett. B **719**(1-3), 103 (2013)
[19] D. P. Stanley and D. Robson, Phys. Rev. D **21**(11), 3180 (1980)
[20] H. T. Ding, X. Gao, A. D. Hanlon *et al.*, Phys. Rev. Lett. **133**(18), 181902 (2024)
[21] C. W. Hwang, Eur. Phys. J. C-Particles and Fields **23**, 585 (2002)
[22] T. Das, (2014), arXiv: 1408.6139
[23] R. J. Hernández-Pinto, L. X. Gutiérrez-Guerrero, A. Bashir *et al.*, Phys. Rev. D **107**(5), 054002 (2023)
[24] C. Patrignani, K. Agashe, G. Aielli *et al.*, Chin. Phys. C **40**, 100001 (2016)
[25] T. Das, D. K. Choudhury, and K. K. Pathak, Indian Journal of Physics **90**, 1307 (2016)
[26] T. Das, K. K. Pathak, and D. K. Choudhury, Int. J. Theor. Phys. **63**(7), 172 (2024)
[27] D. Ebert, R. N. Faustov, and V. O. Galkin, Eur. Phys. J. C **71**, 1 (2011)
[28] L. Adhikari, Y. Li, M. Li *et al.*, Phys. Rev. C **99**(3), 035208 (2019)
[29] A.Höll, A. Krassnigg, P. Maris *et al.*, Phys. Rev. C – Nuclear Physics **71**(6), 065204 (2005)
[30] A. F. Krutov, R. G. Polezhaev, and V. E. Troitsky, Phys. Rev. D **93**(3), 036007 (2016)